Phospholipid Monolayers Supported on Spun Cast Polystyrene Films

John T. Elliott,*[,†,‡] Daniel L. Burden,[§] John T. Woodward,[†] Amit Sehgal,[||] and Jack F. Douglas[||]

Biotechnology Division, Chemical Science and Technology Laboratory, and Polymers Division, Materials Science and Engineering Laboratory, National Institute of Standards and Technology, 100 Bureau Drive, Gaithersburg, Maryland 20899, and Chemistry Department, Wheaton College, Wheaton, Illinois 60817

Received June 12, 2002. In Final Form: November 19, 2002

We investigated the use of spun cast polystyrene (PS) films as a hydrophobic solid support for phospholipid monolayers. Fluorescent microscopy indicated that a 1-palmitoyl-2-oleoyl-*SN*-glycero-3-phosphocholine (POPC) monolayer containing fluorescent lipid formed on ∼80 nm thick films of 2450 M_r PS exposed to phospholipid vesicle solutions. Qualitative fluorescence photobleaching experiments suggested that the phospholipid layer was continuous and the lipid diffusion rate was similar to those observed in glass-supported POPC bilayers. Examination of lipid diffusion by real-time, single-molecule fluorescence detection and fluorescence correlation spectroscopy (FCS) indicated that the lipid diffusion contained multiple components. We interpreted this as being caused by the presence of surface heterogeneities that confine lipid diffusion. In situ atomic force microscopy revealed the presence of 5−20 nm outgrowths on the PS film resulting from surface rearrangement upon exposure of the film to aqueous conditions. It is possible that such rearrangements play a role in determining the lipid translational dynamics. Our studies indicate that PS films can be suitable supports for phospholipid monolayers, but that immersion into an aqueous environment can significantly influence the film topography and the dynamics of the lipid in the supported monolayer.

Introduction

Phospholipid membranes supported on solid substrates are potentially useful for a variety of biological and biotechnological applications.[1−3] They exhibit long-term stability, and the planar geometry of the solid support often simplifies biophysical examination of the lipid membrane with high-resolution microscopies and other surface analytical techniques. Supported membranes have been used to investigate lipid diffusion,[4−6] biomembrane electrical,[7,8] and structural properties,[9,10] protein−phospholipid binding interactions,[11,12] and they have been used as cell surface mimics for the study of antibody-cell surface antigen interactions.[13] These membranes are also promising surfaces for developing new biosensors[14−16] and as biocompatible surface coatings that resist nonspecific protein absorption.[17−19] Many physical properties of the supported membranes are similar to the more commonly used vesicle bilayer system; thus, they are excellent model membranes.

Planar supported lipid membranes are typically constructed by depositing a phospholipid bilayer or monolayer onto a solid support capable of stabilizing the membrane structure. Phospholipid layers can be transferred onto a solid support using Langmuir−Blodgett (LB) techniques,[20] solvent painting,[14] or spontaneous vesicle rearrangement[6] that takes advantage of the self-assembling nature of lipid membranes. The latter technique is convenient since it does not require an LB trough and allows lipid components to be prepared in vesicle form before planar membrane formation.[17,18] The most common supported phospholipid membrane system is prepared by incubating a clean glass surface in a lipid vesicle solution.[4,6] The vesicles reorganize into a planar bilayer structure on the glass, and the lipids exhibit diffusion constants ($\sim 4 \times 10^{-8}$ cm^2/s)[6] similar to those observed in unsupported,[21] vesicular,[22] and biological membranes.[23] Alternatively, a single leaflet of a lipid bilayer can be deposited by vesicle reorganization

* Author to whom correspondence should be addressed. Phone: 301-975-8551. Fax: 301-330-3447. E-mail: jelliott@nist.gov.

† Biotechnology Division, Chemical Science and Technology Laboratory, National Institute of Standards and Technology.

‡ J.T.E., J.T.W., and D.L.B. contributed equally to this work.

§ Chemistry Department, Wheaton College.

|| Polymers Division, Materials Science and Engineering Laboratory, National Institute of Standards and Technology.

(1) Heyse, S.; Stora, T.; Schmid, E.; Lakey, J. H.; Vogel, H. *Biochim. Biophys. Acta* **1998**, *1376*, 319−338.
(2) Sackmann, E. *Science* **1996**, *271*, 43−48.
(3) Groves, J. T.; Boxer, S. G. *Acc. Chem. Res.* **2002**, *35*, 149−157.
(4) Groves, J. T.; Boxer, S. G. *Biophys. J.* **1995**, *69*, 1972−1975.
(5) Schram, V.; Thompson, T. E. *Biophys. J.* **1995**, *69*, 2517−2520.
(6) Kalb, E.; Frey, S.; Tamm, L. K. *Biochim. Biophys. Acta* **1992**, *1103*, 307−316.
(7) Plant, A. L. *Langmuir* **1999**, *15*, 5128−5135.
(8) Steinem, C.; Janshoff, A.; Ulrich, W. P.; Sieber, M.; Galla, H. J. *Biochim. Biophys. Acta* **1996**, *1279*, 169−180.
(9) Frey, S.; Tamm, L. K. *Biophys. J.* **1991**, *60*, 922−930.
(10) Meuse, C. W.; Krueger, S.; Majkrzak, C. F.; Dura, J. A.; Fu, J.; Connor, J. T.; Plant, A. L. *Biophys. J.* **1998**, *74*, 1388−1398.
(11) Cezanne, L.; Lopez, A.; Loste, F.; Parnaud, G.; Saurel, O.; Demange, P.; Tocanne, J. F. *Biochemistry* **1999**, *38*, 2779−2786.
(12) Pearce, K. H.; Hiskey, R. G.; Thompson, N. L. *Biochemistry* **1992**, *31*, 5983−5995.
(13) McConnell, H. M.; Watts, T. H.; Weis, R. M.; Brian, A. A. *Biochim. Biophys. Acta* **1986**, *864*, 95−106.
(14) Cornell, B. A.; Braach-Maksvytis, V. L.; King, L. G.; Osman, P. D.; Raguse, B.; Wieczorek, L.; Pace, R. J. *Nature* **1997**, *387*, 580−583.
(15) Stora, T.; Lakey, J. H.; Vogel, H. *Angew. Chem., Int. Ed.* **1999**, *38*, 389−392.
(16) Stelzle, M.; Weissmuller, G.; Sackmann, E. *J. Phys. Chem.* **1993**, *97*, 2974−2981.
(17) Terrettaz, S.; Stora, T.; Duschl, C.; Vogel, H. *Langmuir* **1993**, *9*, 1361−1369.
(18) Plant, A. L.; Brigham-Burke, M.; Petrella, E. C.; O'Shannessy, D. J. *Anal. Biochem.* **1995**, *226*, 342−348.
(19) Ishihara, K.; Iwasaki, Y. *J. Biomater. Appl.* **1998**, *13*, 111−127.
(20) Tamm, L. K.; McConnell, H. M. *Biophys. J.* **1985**, *47*, 105−113.
(21) Burden, D. L.; Kasianowicz, J. J. *J. Phys. Chem. B* **2000**, *104*, 6103−6107.
(22) Kusba, J.; Li, L.; Gryczynski, I.; Piszczek, G.; Johnson, M.; Lakowicz, J. R. *Biophys. J.* **2002**, *82*, 1358−1372.

10.1021/la0260640 CCC: $25.00
Published on Web 02/11/2003

onto a hydrophobic silanized glass[24,25] or alkanethiol self-assembled monolayers (SAMs) on gold surfaces.[6,7,26] The hydrocarbon nature of the silane and alkanethiol chain monolayers resembles the acyl chains region of a phospholipid leaflet; thus, similar energetic requirements likely stabilize the phospholipid monolayer on the hydrophobic surface.

Phospholipid monolayers can also be supported on hydrophobic polymer beads made from cross-linked polystyrene (styrene divinylbenzene or S-DVB).[27−30] Quantitative evidence for this has been achieved with radioisotope[27,30] and fluorescently labeled phospholipids,[29] and ^{31}P-NMR.[31] The studies indicate that typically one layer of phospholipid coats the bead surface and that the phospholipids are oriented with their hydrophobic acyl chains toward the polymer bead surface.

The fact that phospholipid monolayers can be supported on a hydrophobic polymer is interesting for several reasons: First, phospholipids, which are highly abundant at most biological interfaces, function as excellent biomimetic coatings.[32] Second, the interface between the lipid acyl chains and the styrene surface is significantly different than the mutual acyl chain−chain interface in most supported bilayer systems; it is unclear how this interface would influence dynamic behavior of the phospholipid. Third, the addition of a lipid layer to a polystyrene surface suggests that it may be possible to support phospholipid monolayers on a variety of commercially available polymers used in biotechnology applications. Although the phospholipid coated S-DVB beads have been used in several studies to determine membrane binding constants of phospholipases,[30,33] peptides,[27] and antibodies[34] and as lipobead pH sensors,[29] there has been little effort to further characterize the physical properties (e.g. monolayer continuity and lipid diffusion constants) of a polystyrene supported phospholipid monolayer.

In the studies described here, we considered if spun cast thin unmodified PS films could be used as solid supports for phospholipid monolayers. These films are easy to prepare, are relatively defect free, and have surface characteristics similar to hydrophobic silane and alkanethiol monolayers. We examined vesicle rearrangement and the resulting phospholipid monolayer on the PS film with both conventional fluorescent microscopy and single molecule fluorescence techniques. The identification of single lipid molecules with differing diffusion constants on the same surface provoked us to use in situ atomic force microscopy to identify topology changes that occur in the PS films under aqueous conditions that may be responsible for the heterologous diffusion behavior.

Methods and Materials[35]

General Procedures. All experiments were performed at ∼23 °C unless otherwise indicated. Buffers and rinsing solutions were prepared with npH_2O (Labconco, Kansas City, MI) and were filtered (0.2 μM PES, Nalge Nunc, Rochester, NY). 1-Palmitoyl-2-oleoyl-*SN*-glycero-3-phosphocholine (POPC) and *N*-(nitrobenz-2-oxa-1,3-diazole-4-yl)-1,2-dimyristoyl-*SN*-glycero-3-phosphoethanolamine (NBD-PE) were obtained from Avanti Polar Lipids (Alabaster, AL). *N*-(6-tetramethylrhodaminethiocarbamoyl)-1,2-dihexadecanoyl-*SN*-glycero-3-phosphoethanolamine (TRITC-DHPE) was obtained from Molecular Probes (Eugene, OR). Polystyrene (PS) standards used in these experiments were obtained from Aldrich (St. Louis, MO). Powder free lab gloves (Safeskin Nitrile, San Diego, CA) were used during all handling procedures.

Silicon Wafer Pretreatment. Silicon wafers (75 mm in diameter, 300 mm thick, ⟨100⟩ , Silicon Inc., Boise, ID) were cleaned by immersion into 10% NH_4OH (1 h), followed by rinsing in H_2O and immersion into boiling 10% H_2O_2 in H_2SO_4 (Piranna solution, 2 h). A hydrophobic Si surface was prepared by removal of the SiO_2 layer in 2% HF (15 min). Wafers were then rinsed in water and ethanol, dried with N_2, and used immediately for polymer spin casting.

PS Film Spin Casting and Characterization. Wafers were held onto the spin coater rotor assembly with a vacuum chuck. The wafer surface was covered with filtered toluene (0.2 μM PVDF, Gelman, Ann Arbor, MI) and the wafers were spun at 2000 rpm to remove dust particles. The wafer surface was then covered with a filtered 2450 M_r polystyrene solution in toluene (2% (w/v)), and the wafers were spun at 2000 rpm for 3 min. In cases where the spin lines covered a significant fraction of the film surface, the wafers were cleaned with toluene and the polymer film was recast at a lower acceleration setting. The films were placed under vacuum at room temperature for 24 h for removal of residual solvent and polymer annealing. All films exhibited some heterogeneities due to residual particles on the wafer surfaces or in the polymer solution. Only polymer films with several cm^2 areas free from visible spin lines were used in the vesicle fusion studies.

The advancing contact angles for H_2O on the PS films were determined on a model 110-00-115 goniometer (Rame-Hart Inc., Mountain Lakes, NJ). Film thicknesses were determined by spectroscopic ellipsometry (J. A. Woollam Co., Lincoln, NE). Ellipsometric data were collected between 740 and 600 nm, where the spectrum was not greatly influenced by the thickness of the film. The index of refraction (n) of the PS film was calculated to be 1.57 ± 0.01 when the extinction coefficient (k) for the film was held at 0. This value is in agreement with the accepted value of 1.59 at 20 °C.[36]

Phospholipid Vesicle Preparation. POPC lipid containing 5% NBD-PE or 0.00005% TRITC-PE in chloroform (∼10 mg/mL, 75 μL) was dried in a vial with N_2. Residual chloroform was removed in vacuo for at least 2 h at room temperature. The dried lipid film was dissolved in 2-propanol (30 μL) and was rapidly injected into 10 mM Tris, 100 mM NaCl, pH 7.5 (TNaCl buffer, 2 mL), being vortexed at maximum speed. The solution was vortexed for an additional 1 min after the injection, and vesicle formation was verified by quasi-elastic scattering measurements (Coulter Co., Miami, FL.). This method typically produces small unilamellar vesicles with an average diameter between ∼45 and 70 nm. Vesicles were kept covered in aluminum foil and were discarded after 48 h at room temperature.

Formation of Lipid Monolayers on PS Films. PS-covered wafers were broken into ∼1 × 1 cm pieces and placed in a Teflon holder containing TNaCl buffer and lipid vesicles (0.1 mM final lipid concentration). In some cases, the samples were incubated in the buffer solution for several hours before phospholipid vesicles were added. After 2−8 h at room temperature, the samples were transferred under ∼1 L of npH_2O to a cuvette

(23) Dietrich, C.; Yang, B.; Fujiwara, T.; Kusumi, A.; Jacobson, K. *Biophys. J.* **2002**, *82*, 274−284.
(24) von, T., V.; McConnell, H. M. *Biophys. J.* **1981**, *36*, 421−427.
(25) Subramaniam, S.; Seul, M.; McConnell, H. M. *Proc. Natl. Acad. Sci. U.S.A.* **1986**, *83*, 1169−1173.
(26) Lingler, S.; Rubinstein, I.; Knoll, W.; Offenhausser, A. *Langmuir* **1997**, *13*, 7085−7091.
(27) Retzinger, G. S.; Meredith, S. C.; Lau, S. H.; Kaiser, E. T.; Kezdy, F. J. *Anal. Biochem.* **1985**, *150*, 131−140.
(28) Teegarden, D.; Meredith, S. C.; Sitrin, M. D. *Anal. Biochem.* **1991**, *199*, 293−299.
(29) McNamara, K. P.; Nguyen, T.; Dumitrascu, G.; Ji, J.; Rosenzweig, N.; Rosenzweig, Z. *Anal. Chem.* **2001**, *73*, 3240−3246.
(30) Kim, Y.; Lichtenbergova, L.; Snitko, Y.; Cho, W. *Anal. Biochem.* **1997**, *250*, 109−116.
(31) Stewart, M. W.; Gordon, P. A.; Etches, W. S.; Marusyk, H.; Poppema, S.; Bigam, C.; Sykes, B. *Br. J. Haematol.* **1995**, *90*, 900−905.
(32) Ishihara, K. *Front. Med. Biol. Eng.* **2000**, *10*, 83−95.
(33) Stieglitz, K.; Seaton, B.; Roberts, M. F. *J. Biol. Chem.* **1999**, *274*, 35367−35374.
(34) Drouvalakis, K. A.; Neeson, P. J.; Buchanan, R. R. *Cytometry* **1999**, *36*, 46−51.

(35) Commercial names of materials and apparatus are identified only to specify the experimental procedures. This does not imply a recommendation by NIST, nor does it imply that they are the best available for the purpose.

(36) Brandrup, J. *Polymer Handbook*, 3rd ed.; Brandrup, J., Imergut, E. H., Grulke, E. A., Eds.; John Wiley and Sons: New York, 1999.

fabricated from Teflon. Samples for the epifluorescence microscopy studies were adhered to the cuvette floor with a small amount of silicone grease. Samples used for the confocal microscope studies were firmly mounted to the cuvette by placing the sample under the heads of plastic screws in the cuvette floor. Weakly bound vesicles were removed from the sample surface by gentle pipetting and transferring the cuvette between two different npH_2O wash baths (~2 L each). A cover slip was placed over the sample viewed with the noninverted epifluorescence microscope. Samples used with the confocal microscope were observed with a water-immersion lens; thus, a cover slip was not required. The lipid covered polymer surfaces were not exposed to air during any step in the procedure.

Control glass supported phospholipid bilayers generated by vesicle fusion to acid-cleaned glass coverslips were prepared as previously described.[37] The glass samples were placed into the cuvettes and rinsed with the same procedure used for the PS film substrates.

Conventional Fluorescent Microscopy and Qualitative Fluorescence Photobleaching Experiments. Samples containing NBD-PE lipid were examined with an Olympus BH-2 noninverted fluorescence microscope using 10× or 40× objective lenses. Fluorescence was detected through a Chroma No. 41001 dichroic filter cube (Chroma, Brattleboro, VT), and images were collected with a Quantix CCD camera at −25 °C using IPLab software (Scananalytics, Fairfax, VA). Surface continuity and PS film defects were evaluated by the homogeneity of the fluorescence intensity on the surface. Photobleaching was accomplished by reducing the illumination iris and exposing the fluorescent surface for ~50 s (~1 mm diameter spot on surface). The iris was opened and fluorescence surface images were collected at various time intervals with the source illumination closed between image collection. Time-dependent rounding of the octagonal bleached spot was used as a qualitative indicator of lipid diffusion.[38] The relative lipid concentrations (bilayer or monolayer) on the polymer films or on glass were estimated by quantitative comparison of the fluorescence intensity data collected during an identical interval of time with the same lipid vesicle preparations.[6]

Fluorescence Confocal Microscopy and Single Molecule Dynamics. A cuvette holding a sample containing TRITC-PE lipid was placed on a stage for a confocal microscope constructed as previously described.[21] The confocal detection volume was characterized with a solution of R6G as previously described[21] and was found to have a characteristic beam radius of ~250 nm. Generally, the source (Ar laser) intensity was kept at <50 μW (<25 kW/cm^2) to prevent significant photobleaching of the sample. Co-location of the laser beam waist with the lipid-coated interface was accomplished by slowly moving the substrate in the axial dimension while monitoring single-molecule fluorescent bursts in real time with a multichannel scalar (1 ms bin width). Long, low-amplitude bursts indicated approach of the interface. As fluorescent bursts became apparent, the sample was further raised (~0.75−1.0 μm) to maximize the burst amplitude and minimize the bust duration, thus achieving co-localization. Detector counts were simultaneously sent to an electronic autocorrelator for fluorescence correlation spectroscopy (FCS) analysis. The fraction of immobilized or slowly moving lipid was determined by fitting of the correlated data or by directly analyzing the event durations in the fluorescent burst recordings. The total lipid concentration under the confocal beam was determined by comparing the number of single molecule fluorescent events per unit time observed on the PS supported monolayer to those that were observed on the glass supported bilayer prepared from the identical vesicle solution. Dynamic data were taken at several places on the lipid-coated surface to determine the translational homogeneity.

Atomic Force Microscopy. AFM topographical images of the PS films were collected with a Picoscan AFM (Molecular Imaging) in magnetically driven intermittent contact (MAC) mode. Si cantilevers with a nominal spring constant of 2.2 N/m (Nanosensors) were used for imaging. Samples were mounted under the in situ AFM cuvette and images of the dry samples were collected before the cuvette was filled with water or TNaCl buffer. Once buffer was added, images were collected at various time points to determine the extent to which immersion time influences the surface features. Phospholipid vesicles were typically added to the cuvette after ~5 h, and vesicles were allowed to fuse with the surface for 3 h. AFM images were collected in an attempt to visualize the membrane structure and to determine the effect of the phospholipids on the PS films. In some cases, images were also collected from the samples after they have been submerged for several hours and removed from TKCl buffer or water. Typically several spots on the same sample and on different samples were examined. Average feature descriptions were determined with the Picoscan software or by loading the 2-D images into Scion Image software (Scion Corp., Frederick, MD) and using the image processing functions.

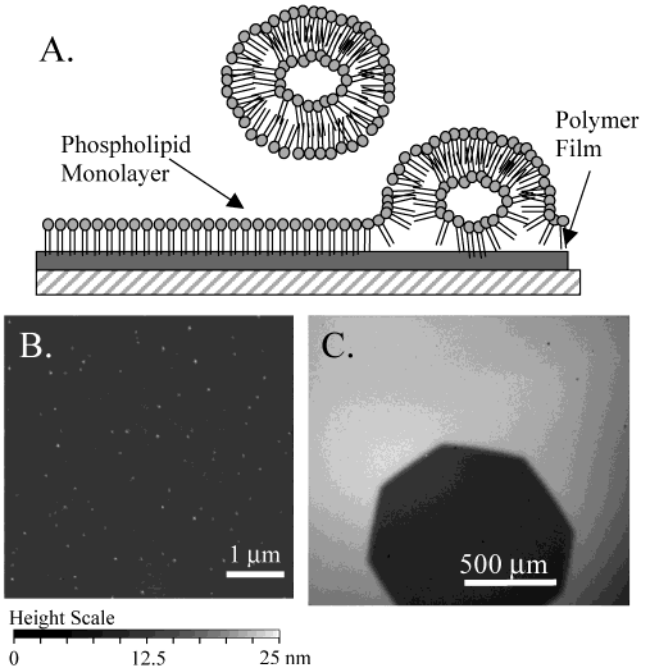

Figure 1. Supporting a phospholipid monolayer on PS films. (A) Expected PL monolayer structure after vesicle fusion to PS films. (B) AFM image of a dry 80 nm thick, 2450 M_r PS film on an HF-etched Si wafer. The overall root mean square surface roughness was typically less than 1.5 nm. The 10 nm high defects (~70 nm in diameter) are likely due to particles in the casting solvent. (C) POPC lipid layer containing 5% fluorescent NBD-PE on the 2450 M_r PS film. Bleaching the fluorescent monolayer with the incident light iris nearly closed formed a 1 mm wide black octagon in the uniform fluorescent field. A few defects are observed as black spots in the upper right side of the image.

Results

Spun cast PS films on silicon wafers are hydrophobic and are typically very smooth (RMS roughness <2 nm) over >25 μm length scales.[39] These features are similar to hydrophobic self-assembled monolayers that are known to induce vesicle lipid rearrangement into phospholipid monolayers.[7] Previous studies with phospholipid monolayers absorbed on styrene−divinylbenzene (S-DVB) beads[27] suggested that it may be possible to form phospholipid monolayers on spun cast polystyrene films (Figure 1A). The molecular features of S-DVB beads differ slightly from the PS spun cast films used in this study. S-DVB is generated from copolymerization of styrene and divinylbenzene monomers and consists of a 3-D network of cross-

(37) Groves, J. T.; Ulman, N.; Boxer, S. G. *Science* **1997**, *275*, 651−653.

(38) Nollert, P.; Kiefer, H.; Jahnig, F. *Biophys. J.* **1995**, *69*, 1447−1455.

(39) Xie, R.; Karim, A.; Douglas, J. F.; Han, X.; Weiss, R. A. *Phys. Rev. Lett.* **1998**, *81*, 1251−1254.

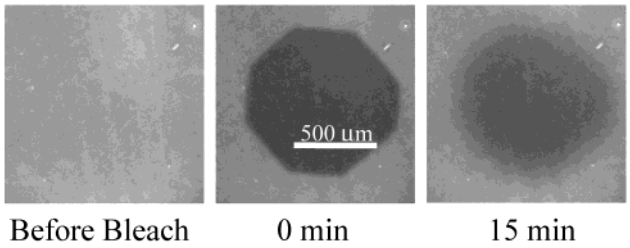

Figure 2. Qualitative fluorescence recovery after photobleaching on a PS supported phospholipid membrane. The fluorescent lipid was bleached by exposing the film to incident light for 1 min with the iris nearly closed. The iris was opened and images were collected at 0 and 15 min. Loss of the octagonal shape and recovery of the fluorescence in the bleached spot indicates that the fluorescent lipid is mobile. The initial recovery rate appeared to be similar to that observed on POPC bilayers on glass (data not shown).

linked polystyrene polymer chains.[40] The spun cast films are stabilized in a glassy state by noncovalent restricted mobility of polymer chains at temperatures less than the bulk PS glass transition temperature (~373 K).[41] We expect that the chemical groups (styrene-like) exhibited on the surface of the beads are similar to those on a spun cast PS film.

PS Film Preparation and AFM Characterization in Air. An ~80 nm thick film of 2450 M_r PS was formed on HF-etched Si wafers. The HF treatment removes the native hydrophilic SiO_2 layer and results in a more favorable interaction between the PS film and the solid substrate. PS films do not dewet from HF-etched wafers at temperatures above the glass transition temperature. The dry spun cast films were smooth with <1.5 nm root mean square roughness for both 1 μm × 1 μm and 5 μm × 5 μm images as measured by AFM. The small defects ranging from 5 to 10 nm high and from 50 to 100 nm wide observed on some surfaces were attributed to undissolved polymer particles or structural features on the underlying etched Si wafer. The water contact angle for the film (95 ± 2°) was in agreement with previously reported values[42] and verified that the film was hydrophobic.

Vesicle Reorganization and Epifluorescence Microscopy Examination of PS Films. The PS film was immersed for several hours in a fluorescent phospholipid vesicle solution, rinsed and examined with conventional epifluorescence microscopy. Micrographs at 10× magnification indicated that the fluorescent lipid was deposited onto to the film and the film exhibited a homogeneous fluorescent intensity (Figure 1C). Small black holes (~5 μm diameter) observed in Figure 1c are likely due to dewetted areas or defects in the PS film.

To distinguish between adhered fluorescent vesicles and a fluorescent phospholipid monolayer resulting from vesicle fusion on the PS film, we used a qualitative fluorescence photobleaching/recovery protocol. The hypothesis for this experiment was that, in contrast to adhered fluorescent vesicles, a continuous monolayer of phospholipid should exhibit uniform phospholipid diffusion and therefore fluorescence that was photobleached should recover as unbleached lipid diffused into the bleached area.[38] A ~1 mm octagonal spot was bleached by exposure to excitation light, and images were subsequently collected over 15 min. As observed in Figure 2, the edge of the octagonal bleached spot becomes more fluorescent over a 15 min time interval, suggesting lipid is diffusing on the surface of the PS film. The extent of fluorescence recovery at this time period was similar to that observed with glass-supported fluorescent bilayers (data not shown), suggesting that the phospholipids deposited on this PS film form a continuous monolayer and have lipid diffusion rates on the order of those observed on glass (~4×10^{-8} cm^2/s for POPC).[6] The nonfluorescent (POPC) lipids used in this study have a gel phase transition temperature of −4 °C and are in a fluid phase at room temperature.[43] Evaluation of the extent of recovery after several hours revealed differences in the PS-supported monolayer and the glass-supported membrane. Near complete recovery was observed on the glass-supported membranes, while a dark center could still be observed on the PS-supported membrane (data not shown). This suggests that a fraction of the phospholipid monolayer absorbed on the PS film exhibited slow diffusion or was relatively immobile.

Table 1. Total Surface Fluorescence Intensity for Supported Fluorescent Phospholipid Membranes

solid support	total surface fluorescence[b]	relative lipid coverage
glass	2490 ± 125	1
2450 M_r PS[a]	1160 ± 30	0.47 ± 0.03

[a] 80 nm film on HF-etched Si wafer. [b] Fluorescent micrographs of 5% NBD-PE in POPC on surface.

Absolute fluorescence intensity comparisons were used to determine the concentration of lipid on the PS film.[6] Although we expected a phospholipid monolayer with acyl chains directed toward the hydrophobic PS surface, it is possible that a bilayer or a multilayer structure is responsible for the photobleaching results. The fluorescence intensity of phospholipid supported on the PS film and a SiO_2 (glass) surface (in arbitrary units) was 1160 ± 30 and 2490 ± 125, respectively (Table 1). Since it is well-established that lipid vesicles reorganize into a bilayer on glass,[37] and the fluorescent intensity on the glass surface is twice that on the PS surface, these data indirectly indicate that a phospholipid monolayer was deposited on the PS surface.[6] These data are consistent with previous studies that show that the equivalent of a phospholipid monolayer can be supported on hydrophobic S-DVB beads.[27,30] Similar results were obtained from the single lipid molecule diffusion data described below.

Lipid Translational Diffusion: FCS and Single-Molecule Analysis. To further examine lipid diffusion on the PS film, we performed real-time fluorescence burst recordings and fluorescence correlation analysis of single lipid molecules on both PS and glass supports. Comparison of the lipid translational dynamics on a PS film to that of a bilayer composed of identical lipids (POPC/0.000005% TRITC-PE) supported on glass underscores the unique behavior of the lipids coating the PS film. Glass-supported bilayers formed from vesicle fusion have been characterized extensively and are known to exhibit approximate homogeneous lipid diffusion.[6,25,44] Our single-molecule recordings and FCS analysis confirm these reports. Figure 3A shows the real-time dynamics of individual lipids from a bilayer on glass. The average event duration is brief (2−5 ms), indicating that the lipids are free to rapidly diffuse across the ~250 nm waist of the confocal beam. Autocorrelation of the data from Figure 3A followed by a

(40) Odian, G. *Principles of Polymerization*, 3rd ed.; John Wiley and Sons: New York, 1991.
(41) Sperling, L. H. *Introduction to Physical Polymer Science*, 2nd ed.; John Wiley and Sons: New York, 1992.
(42) Owen, M. J. In *Physical Properties of Polymers Handbook*; Mark, J. E., Ed.; AIP Press: New York, 1996; Chapter 48.
(43) Marsh, D. *CRC handbook of lipid bilayers*; CRC Press: Boca Raton, FL, 1990.
(44) Salafsky, J.; Groves, J. T.; Boxer, S. G. *Biochemistry* **1996**, *35*, 14773−14781.

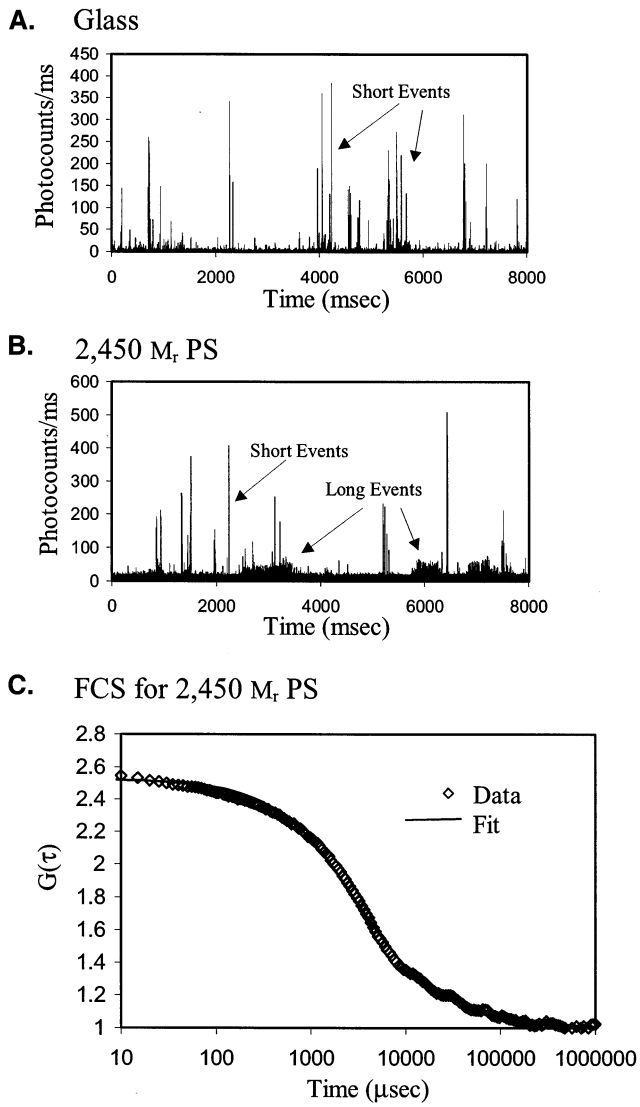

Figure 3. Real-time single fluorescent lipid recordings and fluorescence correlation spectroscopy. A TRITC-DHPE in POPC bilayer or monolayer (1:5 × 10^6) on glass or 2450 M_r PS, respectively, was prepared by incubation in vesicle solution. After rinsing the surface, the lipid diffusion was investigated with confocal microscopy. (A) Real-time recording of TRITC-DHPE molecules diffusing across the confocal beam waist. The predominance of short events suggests that all lipid molecules exhibit rapid diffusion in the POPC matrix. The fluorescence correlation analysis (not shown) using a single component model (eq 2) gives a diffusion constant of (6 ± 1) × 10^{-8} cm^2/s. (B) Real-time recording of lipid molecules diffusing on the 2450 M_r PS film. The presence of short events, similar to those observed on glass, as well as long events indicates that at least two diffusion constants are required to describe the behavior of lipid. (C) Autocorrelation function for lipid diffusion on the 2450 M_r PS film. Data were fit using eq 3 (see text discussion). These data suggest the presence of surface heterogeneities that influence lipid diffusion on the PS film. Analysis of the real-time recordings suggests that ~18% of the lipids exhibit slow translation (see text for discussion).

nonlinear least-squares fit to a one-component diffusion model in two-dimensions[45] enables a lipid diffusion constant to be extracted,

$$G(\tau) = \frac{1}{N}\left(1 + \frac{\tau}{\tau_D}\right)^{-1} + 1 = \frac{1}{N}g_{2D}(\tau) + 1 \qquad (1)$$

where $G(\tau)$ is the autocorrelation function, τ_D is the characteristic lipid crossing time, and N is the time-averaged number of labeled lipids residing within the confocal laser beam. The correlation time (τ_D) and the diffusion constant (D) are related by

$$\tau_D = \omega^2/4D \qquad (2)$$

where ω is the charateristic radius of the laser spot. The single component model fit well to the correlation data (χ^2 = 0.04, fit not shown), yielding a diffusion constant for POPC on glass of (6 ± 1) × 10^{-8} cm^2/s (Table 2). This value agrees with published values determined in other studies.[6,46]

Table 2. TRITC-DHPE Diffusion in Supported POPC Membranes[a]

solid support	no. of fit constants	diffusion constants[b] (cm^2/s)	% total lipid with diffusion constant[b] FCS	% total lipid with diffusion constant[b] real-time event analysis[c]
glass	1[d]	(6 ± 1) × 10^{-8}	100	
2450 M_r PS[e]	2[f]	(5 ± 1) × 10^{-8}	98 ± 1	82
		(4 ± 4) × 10^{-10}	2 ± 0.6	18
2450 M_r PS[e]	2[g]	(5 ± 1) × 10^{-8}	58 ± 4	
		(8 ± 7) × 10^{-10}	42 ± 12	

[a] All uncertainties at 95% confidence interval. [b] Determined with single molecule fluorescence and FCS. [c] Determined by comparing the number of fluorescent events with short and long duration times. [d] Determined by applying eq 1. [e] 80 nm film on HF-etched Si wafer. [f] Determined by applying eq 3. [g] Determined by applying eq 4, α_2 = 0.15.

Figure 3B shows a single-molecule recording of lipid diffusion on the PS film. Narrow bursts (~2−5 ms) similar to those observed for the POPC layer on glass are present, but the data also reveal long-duration fluorescent events (~0.5−1 s). A simple homogeneous diffusion model does not explain this behavior. Assuming the PS film is covered with a lipid monolayer, three possible scenarios that explain this behavior can be considered: (A) continuous lipid motion that is characterized by at least two diffusion constants (some with values more than 100 times less than that found on glass), (B) continuous lipid motion with a single diffusion constant where the lipids may experience sporadic irreversible adsorption events at particular sites on the PS surface, and (C) continuous lipid motion with a single diffusion constant where the lipids may experience reversible adsorption events on the PS surface. Because the TRITC fluorophore emits ~10^5 photons before irreversible photobleaching occurs,[47] rigorous distinction between the latter two possibilities is obscured. A typical lipid might become trapped at a particular site and experience photobleaching, or it might diffuse in and out of a trap on the PS surface before it is photophysically destroyed. In addition, some recordings appear to have long events with low-intensity emission (Figure 3B). These could arise within the context of either scenario B or C, if the adsorption sites are located near the periphery of the laser spot's Gaussian intensity profile. Alternatively, low-intensity events could be explained by an alteration of the label's photophysical rate constants. Unfortunately, the data do not allow unambiguous distinction between these processes.

To account for multiple diffusion components within the framework of scenario A, the two-dimensional auto-

(45) Fahey, P. F.; Koppel, D. E.; Barak, L. S.; Wolf, D. E.; Elson, E. L.; Webb, W. W. *Science* **1977**, *195*, 305−306.
(46) Schutz, G. J.; Schindler, H.; Schmidt, T. *Biophys. J.* **1997**, *73*, 1073−1080.
(47) Soper, S. A.; Nutter, H. L.; Keller, R. A.; Davis, L. M.; Shera, E. B. *Photochem. Photobiol.* **1993**, *57*, 972−977.

correlation function changes to[48]

$$G(\tau) = \frac{1}{N}[(1 - Y)g_{2D_1}(\tau) + Yg_{2D_2}(\tau)] + 1 \qquad (3)$$

where Y is the mole fraction of component 2 in the mixture and $g_{2D_2}(\tau)$ is the correlation function for a second component having a correlation time of τ_{D_2} and diffusion coefficient D_2, as defined in eq 2. This model is valid only if both components have the same quantum yield. Since the possibility of multiple quantum yields between the two diffusing components cannot be ruled out, we also applied a model that includes parameters to account for quantum efficiency differences between components[49]

$$G(\tau) = \sum_{i=1}^{M} \alpha_i^2 \langle N_i \rangle g_{2D_i}(\tau) / [\sum_{i=1}^{M} \alpha_i \langle N_i \rangle]^2 + 1 \qquad (4)$$

where M is the number of diffusing species, $\langle N_i \rangle$ is the average number of molecules of the ith component within the laser, and $\alpha_i = Q_i/Q_1$, where Q_i is defined as a product of absorbance, fluorescence quantum efficiency, and experimental fluorescence collection efficiency of the ith component.

Both eqs 3 and 4 fit the experimental correlation functions extremely well, with a negligible difference in overall appearance ($\chi^2 = 3 \times 10^{-3}$ for both). Figure 3C shows the result from a fit using eq 3, which is virtually indistinguishable from a fit using eq 4. Fitting with eq 3 reveals that a majority of the fluorescent lipid molecules (ca. 98 ± 1%) exhibit a diffusion constant of $(5 \pm 1) \times 10^{-8}$ cm^2/s, a value almost identical to that observed for TRITC-PE in glass-supported POPC bilayers (Table 2). The remainder of the fluorescent lipids (ca. 2 ± 0.6%) exhibit a diffusion constant of $(4 \pm 4) \times 10^{-10}$ cm^2/s. The model including quantum efficiency differences returns a value of 58 ± 4% for the fast component ($D_1 = (5 \pm 1) \times 10^{-8}$ cm^2/s) and 42 ± 12% for the slow component ($D_2 = (8 \pm 7) \times 10^{-10}$ cm^2/s) with $\alpha_2 = 0.15$. Both models suggest that despite the obvious chemical differences between the terminal part of the acyl chains in a bilayer leaflet and the polystyrene chemical structure, part of the phospholipid monolayer is able to freely diffuse at a rate similar to that in a true bilayer membrane. However, the disagreement between the values produced by the two models leaves exact quantification of the slowly moving component somewhat ambiguous.

In an attempt to further probe this discrepancy, we also estimated the fraction of slowly moving or immobilized lipids by direct measurement of individual event durations during the single-molecule time recordings (Table 2). Given the ~250 nm spot radius and the diffusion constant of the fast component ($(5 \pm 1) \times 10^{-8}$ cm^2/s), crossing times should be distributed in a pseudo-exponential fashion[21] with an average of 3−5 ms. From a total of 7675 recorded events, approximately 3976 have durations of less than 5 ms, times consistent with free and unhindered molecular motion. Approximately 712 have durations that range from 50 to 1000 ms, times solely characteristic of the slowly moving or immobilized fraction. The remaining 2987 events lie between the times unique to fast or slow diffusion and contain an undetermined number of each type. Taking a simple ratio of the quantities exclusive to fast and slow components (712/3,976), we estimate that 18% of the phospholipids appear to be slowly moving or immobilized molecules. This value is significantly different from either of the multicomponent correlation models (Table 2). Because FCS analysis is a form of ensemble averaging, the fitting parameters can be biased against small populations of disparate species.[48] Thus, the estimate provided by real-time analysis (i.e., 18% slow component) is likely to be more accurate than the percentages from the correlation models.

The real-time, single-molecule fluorescence recordings can also be used to estimate the percent lipid coverage on the PS film. We prepared glass and PS samples from identical vesicle solutions and made the assumption that the glass supported a perfect bilayer (i.e. two diffusing layers). By simply counting the number of single molecule transits from each surface, we can estimate the percent lipid coverage on the PS film. Using several recordings, we found that the number of events on the PS film was on average 0.46 ± 0.2 of those observed on the glass-supported bilayer, again suggesting the presence of a monolayer of phospholipid on the PS film. These values are consistent with the values measured from the fluorescent intensity of the lipid layers with the epifluorescent microscope (Table 1).

In-Situ AFM Study of a 80 nm, 2450 M_r PS Film. The flat topology of spun cast PS films suggests it is a desirable support for phospholipid monolayers. AFM analysis of the dry films prepared during this study (Figure 1b) indicated that they were very smooth with a root mean square surface roughness of 0.5 nm over a 5 μm × 5 μm image. The results from the single molecule fluorescence studies suggested the presence of surface heterogeneities that influence lipid diffusion rates. We used in-situ AFM to investigate the presence of surface features that may have been induced in the film after immersion into aqueous environments. AFM images of an 80 nm, 2450 M_r PS film before immersion, immersed in aqueous conditions without and with lipid, and after immersion (dried) are shown in Figure 4a−d, respectively. Figure 4b shows that the smooth film undergoes significant surface rearrangement after immersion into aqueous conditions. The features can be described as 5−20 nm high outgrowths approximately 50 nm in diameter, and they are homogeneously distributed over the PS film at a density of ~60/μm^2. They were clearly present in the first AFM scan, suggesting they form within ca. 5 min after immersion into the aqueous solution. In some examples, it appears the outgrowths may have depressions in their centers, but images collected at lower tapping forces suggest that the tapping action of the AFM tip is the likely cause of the apparent depressions. Using a simple geometric model with the outgrowths representing 50 nm hemispheres, the total surface area of the film increases by up to 12% after immersion.

The topological features of the film immersed under aqueous conditions appeared to be stable for at least 6 h since differences in the film were not observed during subsequent AFM imaging scans. Changing the immersion solution from H_2O to TNaCl buffer or POPC vesicle solutions without exposing the surface to air did not produce significant changes in the AFM images. This indicates that the organic buffer molecules (Tris and 2-propanol), salt, and phospholipid did not cause further changes in the thin film surface pattern. We made several attempts to image the phospholipid lipid monolayer structure, but in each case the AFM images before and after phospholipid addition showed outgrowths of similar size and distribution on the surface (compare Figures 4b and 4c). This suggests that the resulting fluid phase POPC monolayer

(48) Meseth, U.; Wohland, T.; Rigler, R.; Vogel, H. *Biophys. J.* **1999**, *76*, 1619−1631.
(49) Wohland, T.; Friedrich, K.; Hovius, R.; Vogel, H. *Biochemistry* **1999**, *38*, 8671−8681.

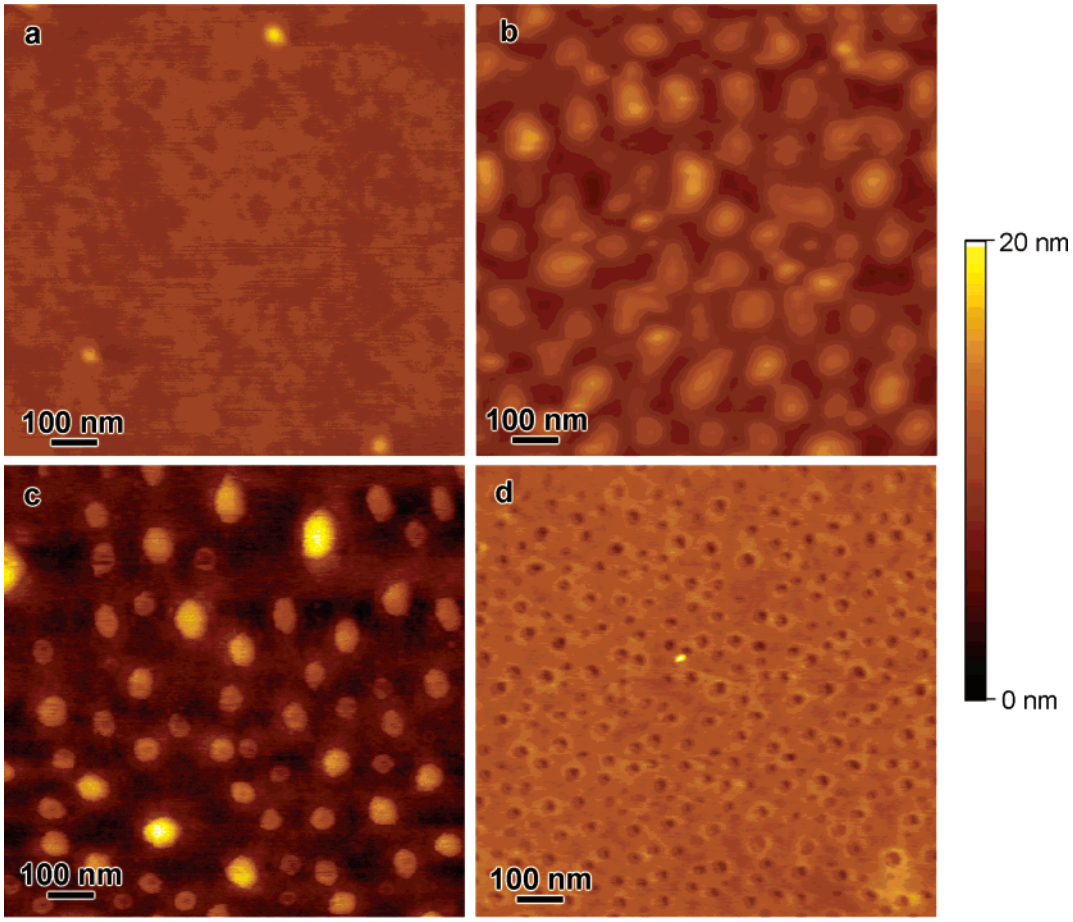

Figure 4. Ex situ and in situ AFM imaging of the 80 nm, 2450 M_r PS film on HF-etched Si substrates. (A) The freshly prepared dried 80 nm thick PS film was smooth. Small, 10 nm high, bumps on the film were likely due to dust or undissolved polymer in the coating solution. (B) When the sample was placed under water, 5−20 nm outgrowths that were 50−100 nm in diameter were observed on the PS film surface. The outgrowths formed immediately upon immersion and remained constant for >8 h. (C) After exposure to the POPC vesicle solution, the outgrowths are still present and tend to give more stable AFM images. New features on the PS film were not observed. This suggests that the breakthrough force of the POPC monolayer is less than the tapping force that was used during imaging. (D) When the PS film was removed from water and dried, 10−20 nm in diameter cavities were observed on the PS film surface. The outgrowths and cavities likely result from extensive surface reorganization after the film is exposed to and removed from water.

has a breakthrough force[50] below the lowest tapping force that was used in these studies (~1 nN) and the AFM tip penetrates the monolayer. In this case, a uniform monolayer of POPC would not significantly increase the height of the outgrowths, but it may add several nanometers to the measured width of the outgrowths. We actually tend to see slightly smaller and more sharply resolved outgrowths after adding lipid to the PS films. It is not clear if the differences in the AFM images are due to real changes in the PS film topography or are a result of alterations in the physical forces between the AFM tip and the PS film in the absence or presence of a phospholipid monolayer.

Interestingly, removal of the PS film from water resulted in a film with 10−20 nm cavities (Figure 4d). The density of cavities are 3-fold greater than those observed for the outgrowths. The depth of the cavities could not be measured due to the AFM tip dimensions; thus, it is not clear if the holes extend completely to the Si substrate.

We used in-situ ellipsometry[51] to evaluate the time course for bulk film changes under an aqueous environment (data not shown). However, we were not able to observe the rapid increase in thickness due to the PS rearrangement and formation of outgrowths (the first measurement was after 2 min), but we were able to observe a slow change in thickness (~15 Å) over a 15 h time period. These data suggests that film rearrangements due to water immersion were complete after 15 h. In general, the surfaces used in the single molecule fluorescence studies were incubated in vesicle solutions for 3−6 h and examined for 2−4 h. Obvious differences in lipid dynamics were not observed between these samples. This result was also reflected in the fluorescence photobleaching studies that indicated that preincubation of the PS film in buffer for several hours before vesicle fusion resulted in homogeneous fluorescent films on which fluorescence photobleaching and recovery was observed.

Discussion

In principle, the formation of phospholipid monolayers on a polymer surface would be a relatively simple way to make a polymer film biocompatible for a variety of biotechnology applications and for making model biomimetic layers for in vitro studies. Spun cast PS films are very smooth and have hydrophobic surface properties similar to silane and alkanethiol self-assembled mono-

(50) Schneider, J.; Dufrene, Y. F.; Barger, W. R.; Lee, G. U. *Biophys. J.* **2000**, *79*, 1107−1118.

(51) Reipa, V.; Gaigalas, A. K.; Vilker, V. L. *Langmuir* **1997**, *13*, 3508−3514.

layers that are known to induce vesicle lipid rearrangement into phospholipid monolayers.[6,24] This suggests that the cast PS films may also be suitable lipid monolayer supports. We examined the process of vesicle reorganization at this hydrophobic polymer surface to determine if it is analogous to the convenient method for adding lipid monolayers to hydrophobic silane and alkanethiol self-assembled monolayers. Our results suggest that this is indeed the case.

The results from conventional and confocal fluorescent microscopy techniques indicate that approximately one monolayer of phospholipid is adsorbed to the PS film and that on average the phospholipids diffuse at rates similar to those observed in glass-supported phospholipid bilayers. This is an interesting result because of the large difference in the nature of chemical groups present at the phospholipid monolayer leaflet interface. The glass supported bilayer and the silane and alkanethiol supported monolayers have terminal alkane groups at the lipid leaflet interface. The PS lipid support exhibits mainly benzyl groups at the leaflet interface. The difference in the chemical nature of the surface is also reflected in the water contact angle for the PS film, which is 10−15° less than that observed on silane and alkanethiol SAMs. Although we cannot predict how interfacial chemical differences will influence either the dynamics or stability of the supported lipid monolayer, these data suggest that a variety of hydrophobic polymers with different chemistries may be able to support phospholipid monolayers. It is also interesting to note that we know of two hydrophobic polymers in which PL monolayer addition by vesicle reorganization does not occur. We found the fluorescent PL monolayers did not form on spun cast polybutadiene (2800 M_r) films (data not shown), and work by others indicates that vesicle reorganization does not occur at Teflon surfaces.[38] It is not clear if these surfaces prevent the initial vesicle adsorption process or do not present sufficient driving force for vesicle lipid reorganization. However, it does suggest that PL monolayer formation on a hydrophobic surface may have particular chemical and topographical requirements.

Phospholipid diffusion on the PS film was subjected to single molecule analysis to examine the dynamic behavior of individual lipid molecules in the monolayer. Autocorrelation of the single molecule event recordings indicated that 98% of the lipids diffused at a rate similar to that observed on glass-supported PL bilayers (Table 2). The real time recordings revealed the presence of longer low-intensity fluorescence bursts, indicating the presence of lipid (18%) diffusing at a rate that was 2-orders of magnitude less than that for the faster component (Figure 3B, Table 3). Slower moving or immobile lipid fractions have also been observed on a variety of phospholipid monolayers and bilayers on solid supports.[6,46,52] These results suggest the presence of adsorption sites or defects on the PS film that can influence the dynamic motion of the individual lipid molecules.

In an attempt to identify structures in the PS film that may act as lipid adsorption sites, we examined the PS film in aqueous environments with in situ AFM. Initially, we expected the presence of defects in the film that may have resulted from localized dewetting around microscopic defect areas in the Si substrate. Surprisingly, we found the whole film rapidly undergoes significant surface rearrangement culminating in small outgrowths homogeneously distributed over the film surface. We observed outgrowths on PS films with molecular weights varying from between 2450 and 100 000 and film thicknesses between 80 and 200 nm. In addition, the outgrowths were observed on films cast onto substrates with Si, SiO_2, and Au surface coatings, indicating that the energetic forces between the substrate and polymer film do not contribute to the surface patterning mechanism (data not shown). For the case of the PS film cast onto the SiO_2 covered wafer, the outgrowths were observed on top of larger bulges resulting from polymer film dewetting from the substrate under aqueous conditions. These results suggest that the outgrowths result mainly from forces that develop at the PS film and aqueous interface. An osmotically driven blistering process similar to the one described for spun cast films of poly(D,L-lactide) under aqueous conditions may be responsible for the formation of the outgrowths we observed in this study.[53]

We attempted to identify structural features in the POPC lipid layer with AFM, but we did not observe any significant differences in the AFM images before and after phospholipid vesicle addition (compare Figures 4b and 4c). We used POPC phospholipids in this study since they have a liquid to gel phase transition temperature at −4 °C and the lipids exhibit free diffusion at room temperature. The fact that we did not observe any significant changes in the AFM images of the PS film after vesicle addition and monolayer formation was not completely unexpected as it has been shown that the AFM tip can completely penetrate liquid crystalline lipid phases even under low tapping forces.[50,54] For example, while determining the mechanism that causes topographical height differences between phases in phase-separated DOPE/DSPE lipid bilayers, Schneider et al. found that the thickness of the liquid-phase DOPE bilayer is only ∼1.6 nm instead of 6.1 nm measured for DSPE gel-phase bilayer.[50] Subsequent studies with asymmetric DOPE/DSPE bilayers suggested that this is due to the AFM tip deforming the liquid crystalline layer. It is likely that a similar effect occurs when probing the PS-supported POPC monolayer. Although numerous studies describing bilayer and monolayer structures through AFM imaging have been reported, many utilize lipids with gel-phase properties[55,56] or mixed lipids systems to visualize contrast between lipid phases,[50] or they used contact mode "scraping" to remove a portion of the lipid coating to generate topographical contrast.[55,57] Since these contrast mechanisms were not available in our experimental system, it is unclear what topographical features we would observe for the binary POPC monolayer. The absence of new structural features on the PS film after phospholipid addition does indicate that solid aggregates resulting from a nonspecific lipid−polystyrene interaction are not present, but it does not define the source of the slowly moving lipid fraction we observed on the polymer film. Future studies of lipid monolayers on polymer films that utilize lipids in a gel phase may allow AFM imaging of the phospholipid monolayer structure.

We also found that removal of thin PS films (80 nm) from the aqueous environment resulted in the formation of cavities, but these cavities were not observed in the thicker 200 nm films (data not shown). This suggests the

(52) Kuhner, M.; Tampe, R.; Sackmann, E. *Biophys. J.* **1994**, *67*, 217−226.

(53) Sharp, J. S.; Jones, R. A. L. *Adv. Mater.* **2002**, *14*, 799−802.

(54) Dufrene, Y. F.; Boland, T.; Schneider, J. W.; Barger, W. R.; Lee, G. U. *Faraday Discuss.* **1998**, *111*, 79−94.

(55) Kumar, S.; Hoh, J. H. *Langmuir* **2000**, *16*, 9936−9940.

(56) Rinia, H. A.; Boots, J. W.; Rijkers, D. T.; Kik, R. A.; Snel, M. M.; Demel, R. A.; Killian, J. A.; van der Eerden, J. P.; de Kruijff, B. *Biochemistry* **2002**, *41*, 2814−2824.

(57) Steinem, C.; Galla, H. J.; Janshoff, A. *Phys. Chem. Chem. Phys.* **2000**, *2*, 4580−4585.

cavities result from redistribution of the limited quantity of PS material on the thin film during the drying process.

It is unclear if the outgrowths in the PS film or undefined structural features in the POPC monolayer are responsible for the lipid dynamics observed by the single molecule fluorescence experiments. The fact that the outgrowths are observed on greater than 12% of the surface and up to 18% of the lipid exhibits low diffusion constants suggests that the PS outgrowths may be involved in confining lipid diffusion. Further investigations targeted at correlating surface topology and lipid dynamics are necessary to confirm this hypothesis.

Conclusion

Our data indicate that phospholipid monolayers can be supported on spun cast PS films. This may be useful for developing biotechnology devices because it provides a simple method to make the polymer surface biocompatible, and it provides a method to introduce biospecific molecules onto the surface. Previous studies have "decorated" supported phospholipid monolayers with lipids conjugated to peptides,[58] proteins,[59,60] and sugar[61] groups. Bioactive groups may be easily introduced on the surface of PS films via vesicle fusion with vesicles containing the appropriate functionalized lipid. The natural protein adsorption resistant nature of the phospholipid membrane is also a desirable feature as it may act to reduce nonspecific adsorption of proteins to hydrophobic polymers.[17,18] The lipid-coated PS films may be useful in biosensors for protein−protein or protein−membrane interactions. In addition, polymer films functionalized with phospholipid monolayers may be useful in tissue engineering studies that examine the influence of chemical cues on cell growth and phenotype.[62]

An unanticipated finding of these spun cast PS films is that they undergo an unusual surface pattern formation when exposed to aqueous solutions. These patterns collapse upon drying, and on thin films (∼80 nm), the collapse leads to the formation of cavities. Polymer film characterization during and after exposure to aqueous conditions is critical if the topographical properties of the film are important for a specific biotechnology application. For example, a previous study described cell growth on spun cast PS films.[63] Although the surfaces were characterized under dry conditions, depending on how the film was handled, the film topology ultimately presented to the cell may not be identical to that initially observed. In the case of cell growth, where cells may be responsive to nanoscale structure features in the surface,[64] patterns such as those shown in Figures 4b and 4d may impact the experimental outcome.

Chemical and photoinitiated cross-linking polymers such as epoxies and PMMA polymer films may exhibit minimal surface rearrangements under aqueous conditions, and preliminary results suggest these materials may function as hydrophobic supports for PL monolayers. We envision that further studies with hydrophobic polymer-supported lipid monolayers prepared by this simple vesicle-based method may help to expand the use of these polymer in biotechnology applications.

Acknowledgment. We would like to thank Dr. Peter Barker for use of his epifluorescent microscope and CCD camera. We would also like to thank Curt Meuse for valuable discussions, and Steven Poppen and Emily Rupp for assistance with data analysis. D.L.B. acknowledges the Wheaton College Alumni Association, the Camille and Henry Dreyfus Faculty Start-up Grant Program for Undergraduate Institutions and the donors of the Petroleum Research Fund, administered by the American Chemical Society, for support of this research. J.T.E. acknowledges the National Research Council and NIST for fellowship support.

LA0260640

(58) Cooper, M. A.; Try, A. C.; Carroll, J.; Ellar, D. J.; Williams, D. H. *BBA-Biomembranes* **1998**, *1373*, 101−111.

(59) Cooper, M. A.; Williams, D. H. *Anal. Biochem.* **1999**, *276*, 36−47.

(60) Liley, M.; Bouvier, J.; Vogel, H. *J. Colloid Interface Sci.* **1997**, *194*, 53−58.

(61) Reed, R. A.; Mattai, J.; Shipley, G. G. *Biochemistry* **1987**, *26*, 824−832.

(62) Groves, J. T.; Mahal, L. K.; Bertozzi, C. R. *Langmuir* **2001**, *17*, 5129−5133.

(63) Walboomers, X. F.; Monaghan, W.; Curtis, A. S.; Jansen, J. A. *J. Biomed. Mater. Res.* **1999**, *46*, 212−220.

(64) Curtis, A.; Wilkinson, C. *Biochem. Soc. Symp.* **1999**, *65*, 15−26.